Geological Society of America
Special Paper 358
2002

Transition tectonics of northern Taiwan induced by convergence and trench retreat

Jyr-Ching Hu
Shui-Beih Yu
Institute of Earth Sciences, Academia Sinica, P.O. Box 1-55, Nankang, Taipei, Taiwan, Republic of China
Hao-Tsu Chu
Central Geological Survey, PO Box 968, Taipei, Taiwan, Republic of China
Jacques Angelier
Tectonique Quantitative, URA 1315, CNRS, Université Pierre et Marie Curie, 4 place Jussieu, T26, E-1, 75252 Paris Cedex 05, France

ABSTRACT

As an active collision zone between the Luzon arc and the China continental margin, the Taiwan mountain belt is undergoing strong crustal shortening and rapid uplift, especially in its south-central part. In contrast, northeast Taiwan, located near the junction between the Taiwan orogen and the Ryukyu arc, is subject to both the compressional force exerted by the indentation of Philippine Sea plate and the tensile force induced by trench retreat related to the suction force at the Ryukyu Trench. As a function of these two forces, the stress regime rapidly changes from south to north, from compression in the Taiwan collision zone to extension in the Ryukyu subduction zone. By using a two-dimensional plane-stress finite-element model with elasto-plastic rheologies, we analyze the relationship between the kinematics of convergence, the crustal deformation, and the stress distribution in the present Taiwan collision zone between the Ryukyu and Luzon subduction zones. Our model predicts that in northeastern Taiwan, a transition zone may develop between pure compression (which characterizes most of the collision zone of Taiwan) and pure extension (which prevails in the northeastern part of the model). The transition in the stress field is characterized by two intermediate regimes, one mainly compressional and one mainly extensional, where significant strike-slip deformation is expected. We show that the interaction between the opening of the Okinawa Trough and the collision at the northwestern boundary of the Philippine Sea plate plays a crucial role in controlling the stress and strain patterns. The location of the transition zone in the north is a balance between these two factors, which may explain the variability of tectonic regimes in the region.

INTRODUCTION

The island of Taiwan is located at the junction of the Ryukyu arc and the Luzon arc at the western edge of the Philippine Sea plate. The plate interaction around this segment of the convergent plate boundary between the Eurasian and Philippine Sea plates is complex (Fig. 1). Seismicity northeast of Taiwan indicates the presence of a Wadati-Benioff zone, where the Philippine Sea plate subducts northward along the Ryukyu Trench (e.g., Tsai, 1986). In contrast, south of Taiwan, the Eurasian plate subducts southeastward beneath the Philippine Sea plate along the Manila Trench (e.g., Wu, 1978; Tsai, 1986; Pezzopane

Hu, J.-C., Yu, S.-B., Chu, H.-T., and Angelier, J., 2002, Transition tectonics of northern Taiwan induced by convergence and trench retreat, *in* Byrne, T.B., and Liu, C.-S., eds., Geology and Geophysics of an Arc-Continent collision, Taiwan, Republic of China: Boulder, Colorado, Geological Society of America Special Paper 358, p. 149–162.

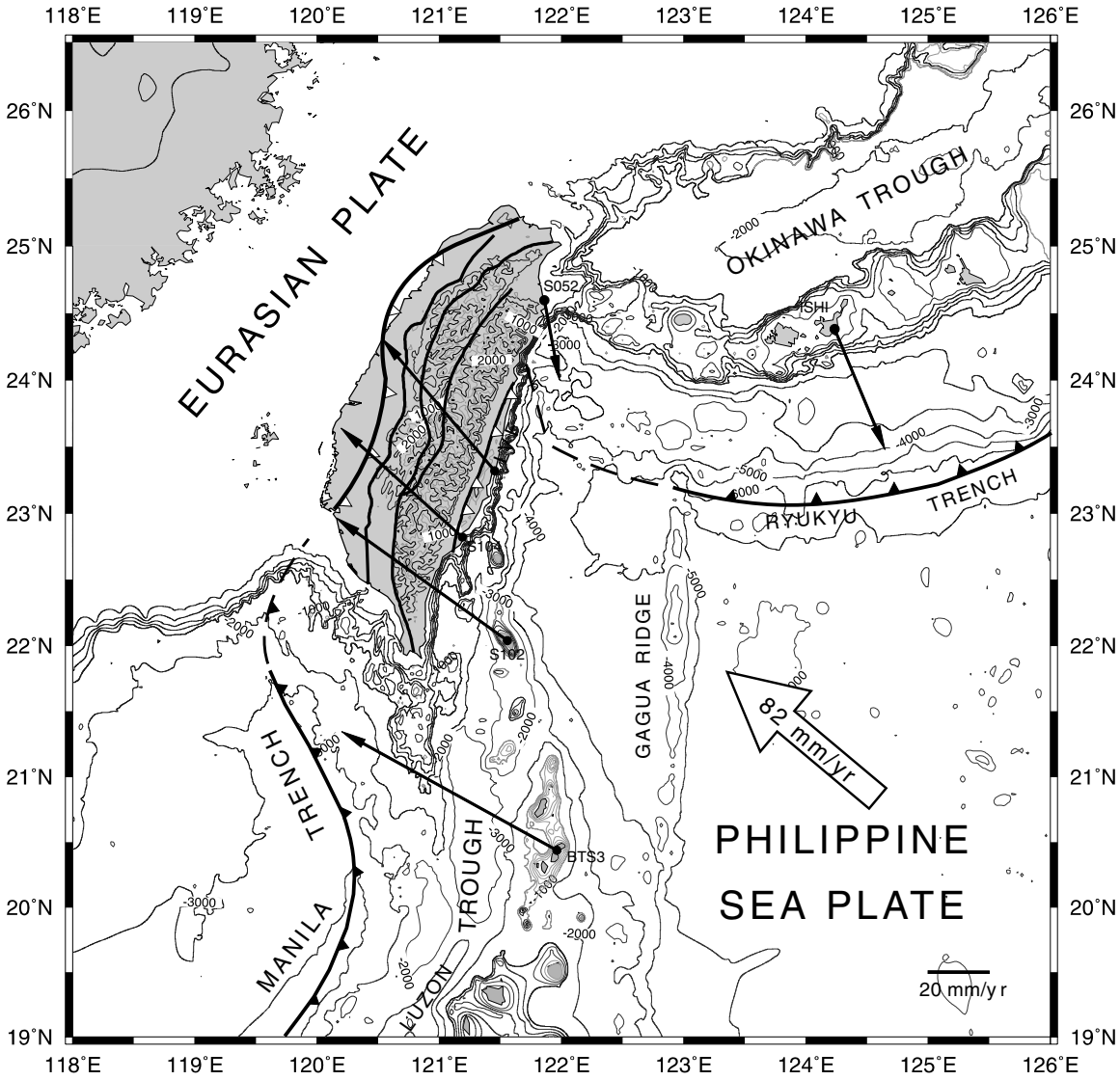

Figure 1. Bathymetric and geodynamic map of the vicinity of Taiwan. Subduction along the Ryukyu and Manila Trenches is represented with closed barbs on the overriding plate. The Longitudinal Valley fault (LVF) strikes northward along the East Coast and shows both oblique left-lateral and reverse (open barbs on hanging wall) movement (e.g., Barrier, 1985). Large open arrow and number indicate the relative-plate-motion vector between the Philippine Sea and Eurasian plates as determined by Yu et al. (1997). GPS velocity vectors relative to Paisha station (Penghu) appear as thin arrows. The data of ISHI station at Ishigaki in the Ryukyu Islands are provided by ERI (Earthquake Research Institute).

and Wesnousky, 1989). The Taiwan collision zone thus marks a segment of plate boundary where subduction undergoes a polarity reversal. Furthermore, Taiwan is where the Luzon arc initially collided with the Eurasian continent at ca. 5 Ma (e.g., Ho, 1986; Angelier, 1990; Teng, 1990; 1996). The fold-and-thrust belt of Taiwan advanced northwestward, while the orogen growth was propagating southwestward along the passive continental margin of the Eurasian plate (Suppe, 1984). As an active collision zone between the Luzon arc and the China continental margin, the Taiwan mountain belt, particularly its south-central part, is undergoing strong crustal shortening (e.g., Yu and Chen, 1994) and rapid uplift (e.g., Liew et al., 1990; Liu and Yu, 1990; Wang and Burnett, 1990; Pirazzoli et al., 1993).

Extensive paleostress analyses have been made throughout the island of Taiwan since 1984; thus the evolution of tectonic paleostresses is well known in terms of regional distribution and major trends (Barrier, 1985, 1986; Barrier and Angelier, 1986; Angelier et al., 1986, 1990; Lee, 1986; Lee and Wang, 1988; Chu, 1990; Rocher et al., 1996; Lacombe et al., 1997). These paleostress determinations allowed not only description of local mechanisms, but also understanding of the regional

tectonic patterns at the scale of the plates. The regional knowledge of the late Cenozoic paleostress field thus provided strong constraints in the geodynamic interpretation of the Taiwan collision belt. In order to address the problem of consistency between paleostress and deformation, and taking advantage of these constraints, several numerical experiments considering strain-stress relationships were carried out (e.g., Huchon et al., 1986; Hu et al., 1996). These experiments aimed to evaluate the general compatibility of the kinematic boundary conditions, the geologic structure, rheology, and paleostress patterns (Hu et al., 1996, 1997).

During the past few years, the Global Positioning System (GPS) became one of the most important geodetic tools for studying crustal deformation (e.g., Dixon, 1991). In Taiwan, accurate relative positioning with the GPS in a dense network allowed description of crustal deformation at the scale of the collision belt and surrounding island (Yu and Chen, 1994). To better quantify both the rate and style of deformation currently taking place along the complex convergent plate boundary of Taiwan, the 131 stations of the "Taiwan GPS Network" were surveyed four to six times from 1990 to 1996 with dual-frequency geodetic receivers (Yu et al., 1997). Such accurate geodetic data on present-day deformation thus provided new opportunities to study the relationships between the crustal deformation and the plate kinematics. It became possible to describe not only the type and orientation, but also the magnitudes of tectonic effects, by using GPS-based displacement data rather than just the paleostress orientation data as constraints in modeling (Hu et al., 1997).

In this paper, we aim to characterize the crustal deformation in northern Taiwan induced by the Taiwan collision and surrounding subduction zones. In the westernmost Ryukyu-Taiwan region, the rapid change from oblique subduction to collision is most intriguing because it involves all major seismogenic structures and is accomplished in a very short distance. The relationship among structures showing different patterns of crustal strain provides fundamental constraints on the accommodation of deformation along the subduction-collision transition. We combine numerical simulation, deformation data from GPS studies, and geologic constraints in order to better quantify the rate, style, and distribution of deformation currently taking place along the complex oblique subduction to collision boundary of northern Taiwan.

TECTONIC SETTING

The island of Taiwan is located along a segment of the convergent boundary between the Philippine Sea plate and Eurasia plate, where collision and subduction processes occur (Fig. 1). The Philippine Sea plate moves in a northwest direction and subducts beneath Eurasia along the Ryukyu Trench, but flips subduction polarity and overrides the Eurasia plate along the Manila Trench (Fig. 1). The southeast-facing Ryukyu arc-and-trench system extends from southern Kyushu (Japan) to east of Taiwan. The morphology of the Ryukyu Trench disappears west of 123°E where it is intercepted by the Gagua Ridge (Fig. 1). This subduction zone is associated with the backarc spreading in the Okinawa Trough, which ends in the Ilan Plain of northeastern Taiwan (Fig. 1) (Tsai, 1986). In contrast, the west-facing Luzon-Manila arc-and-trench system extends from the Philippines to about 22°N (Fig. 1). North of 22°N, the bathymetric signature of the Manila Trench disappears and the Manila Trench–Luzon arc system gradually loses its identity as it gets close to the continental margin of southeast China. The Manila Trench system extends onshore in southeastern Taiwan and forms the Quaternary fold-and-thrust belt of southern Taiwan (Liu et al., 1997). At present, the collisional process is still active in southern and central Taiwan as demonstrated by the crustal shortening and intense seismicity (e.g., Wu, 1978; Tsai, 1986; Yu and Chen, 1994).

A characteristic feature of the Taiwan mountain belt is the major change in the general structural trends between central Taiwan and northern Taiwan. On average, the mountain ranges in central Taiwan trend north-northeast south of 24.5°N, whereas in northeastern Taiwan they trend east-northeast (Suppe, 1984; Angelier et al., 1990). The existence of major change in structural trends of about 55° between 24°N and 25°N (Fig. 2) has been interpreted to be the result of subduction flipping and opening of the Okinawa Trough (Suppe, 1984).

In contrast with south-central Taiwan, northeast Taiwan has undergone postcollisional processes and has been incorporated in the southern Ryukyu arc system. Evidence for this late evolution is provided by the presence of Quaternary extensional structures (Lee and Wang, 1988; Lu et al. 1995) and extensional earthquake focal mechanisms (Tsai et al., 1977; Tsai, 1986; Yeh et al., 1991; Kao et al., 1998). All of these features indicate that the polarity of subduction has flipped in northern Taiwan; accordingly, the compressional tectonism that resulted in the growth of the Taiwan orogen has been replaced by the extensional tectonism of the Okinawa Trough (Suppe, 1984; Lee and Wang, 1988; Teng, 1996). On the basis of integration of available radiometric age data, Teng et al. (1992) pointed out a westward-younging character for the volcanism in northern Taiwan. It appears that both the onset and the cessation of the calc-alkalic volcanic activity migrated from east to west near the western tip of the Ryukyu arc in northern Taiwan. Teng et al. (1992) proposed that the arc magmatism was initiated by the westward encroachment of the Ryukyu subduction system and ceased subsequently as a result of the southwestward propagation of the opening of the Okinawa Trough. Therefore, the emplacement of the ultrapotassic rock may have resulted from the onset of postcollision extension, as recently claimed on the basis of geochemical studies (Chung et al., 1995; Chen et al., 1995).

The east-northeast-trending belt segment of northeastern Taiwan is composed of several stratigraphic units, which belong to the northern Hsüehshan Range, the Western Foothills, the Coastal Plain, and the Pleistocene volcanic rocks (Fig. 3a). In

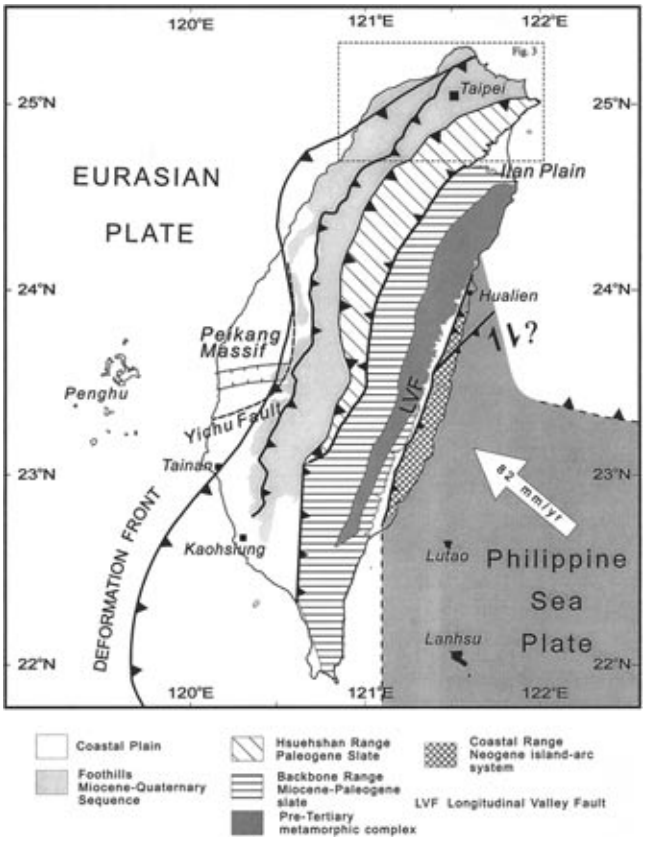

Figure 2. Tectonic framework and main structural units in Taiwan. Main tectonic units follow Ho (1986) and Biq, (1989). Major thrust faults have triangles on the hanging wall.

the Coastal Plain and Western Foothills, clastic sedimentary rocks crop out, with ages ranging from Oligocene to Quaternary. The Hsüehshan Range (Fig. 2) includes a passive-margin shallow-marine sequence of Eocene to Oligocene age that is folded and metamorphosed. Metamorphic grades increase from northwest to southeast, from unmetamorphosed or slightly metamorphosed rocks in the Coastal Plain area to lower-greenschist facies in the inner Hsüehshan Range. Studies in the northern Hsüehshan Range (Lu et al., 1995) show that it was subject to complex deformation processes including contraction, regional horizontal bending, transcurrent faulting, block rotation, and extension. The structural analyses in central and northern Taiwan indicate that during the late Cenozoic, the Hsüehshan Range underwent a pop-up style of deformation (Clark et al., 1993).

The late Cenozoic structure of northern Taiwan (Fig. 3) is characterized by numerous northeast-trending folds and thrust faults, which are deformed by broadly spaced strike-slip faults and some normal-fault systems. There is a slight obliquity between the regional trends of the major thrust units and the fold axes, revealing a poorly marked en echelon arrangement of several folds and thrusts between Taipei and Keelung. Pliocene–Quaternary normal faults are present in several basins and depression structures within the compressional mountain chain, like the Taipei Basin, the Ilan Basin, and the Yenliao depression together with the Chinkuashih gold-copper field (Fig. 3A). Extensional structures widely cut across the old contractional structures and are thought to be associated with downfaulting of Quaternary intramontane basins (Lee and Wang, 1988).

Recent studies of fault-slip data sets (e.g., Lu et al., 1995), borehole breakouts (Suppe et al., 1985), and focal mechanisms of earthquakes (Yeh et al., 1991) have shown that north-south and east-west extensional movements are common throughout northernmost Taiwan and the Ilan Plain area. According to most analyses, north-south extension dominates near the western tip of the Okinawa Trough (e.g., Ilan Plain and adjacent offshore areas), whereas east-west extension prevails in northernmost Taiwan (e.g., Taipei basin and the Tatung volcano field, see Fig. 3). To the east, the north-south extension is widespread in the Ryukyu arc and corresponds to backarc spreading activity of the Okinawa Trough. The Okinawa Trough shows various extensional features including grabens identified from regional bathymetry and seismic reflection profiles (e.g., Kimura, 1985; Sibuet et al., 1987, 1998; Sato et al., 1994) as well as earthquake focal mechanisms (e.g., Kao and Chen, 1991). In addition, geodetic and tomographic studies suggest that the extension associated with the opening of the Okinawa Trough extends westward beneath northeast Taiwan (e.g., Yeh et al., 1989; Liu, 1995).

STRESS AND STRAIN PATTERNS IN NORTHERN TAIWAN

Present-day stress and paleostresses related to Pliocene–Quaternary collision

Although it is not described in detail hereafter, the distribution of recent and present-day tectonic stress patterns provides an important key for understanding the recent deformation in northern Taiwan. On the basis of the results of several studies, the paleostresses are summarized in Figure 3B in terms of trends of the maximum horizontal compressional stress axes (σ_1) corresponding to different compressional structures, including thrusts, strike-slip faults, fracture cleavages, folds, and joints (Lu et al., 1995). Considering the dispersion due to uncertainties of measurements and paleostress determinations, the variations of σ_1 trends cannot be simply accounted for by the natural irregularities and stress-field inhomogeneity related to a single event affecting a rigid mass. In addition, these Pliocene–Quaternary patterns of compressional stress related to collision cannot be considered as a whole because it has been demonstrated that significant changes have occurred over time. For example, the late Pliocene–Pleistocene records of compressional paleostresses could be separated into two principal tectonic events, as proposed by Angelier et al. (1986). Further detailed analyses, especially in the Hsüehshan Range in northern Taiwan (Angelier et al., 1990) have revealed a complex set

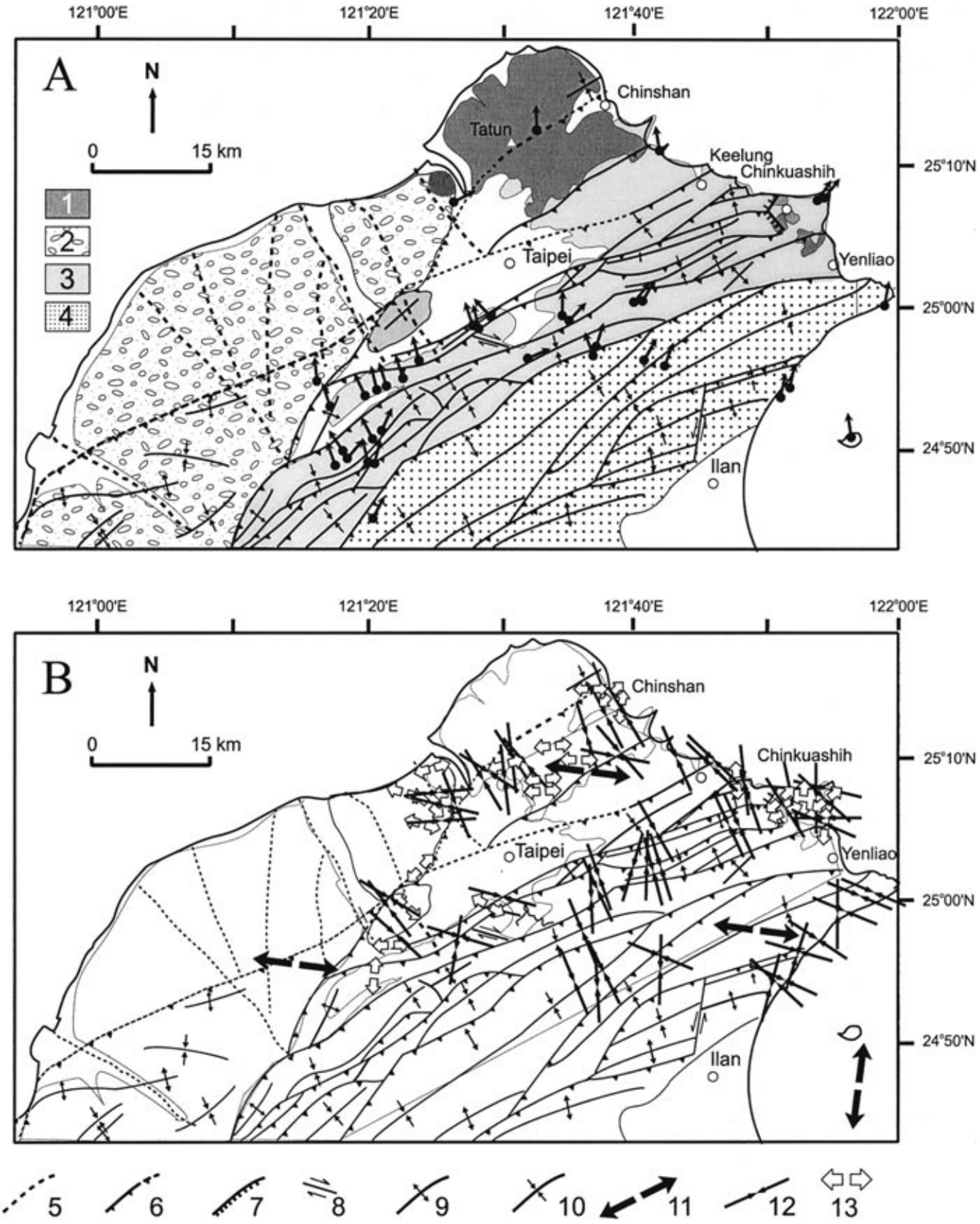

Figure 3. Location map showing general geologic structures interpreted from the geologic maps (Ho, 1986) and SLAR (side-looking airborne radar) image of northern Taiwan (Mars Inc., 1981). Keys: 1—Pleistocene volcanic rocks, 2—Pleistocene conglomerate, 3—Western Foothills, 4—Hsüehshan Range, 5—major fracture, 6—thrust fault, 7—strike-slip fault, 8—normal fault, 9—anticline axis, 10—syncline axis, 11—extension based on focal mechanism, 12—compression, 13—extension based on normal faults (modified after Lu et al., 1995). (A) Small dots with arrows describe the declinations of magnetic fabrics in the rocks of northeastern Taiwan (after Lue et al., 1991). (B) Summary of the results of the paleostress analyses. For extension, each pair of divergent arrows (local trend of σ_3) corresponds to the analysis of normal faults and focal mechanism. For compression, each pair of convergent solid arrows (local trend of σ_1) corresponds to the analysis of a site with many compressional structures, including thrusts, strike-slip faults, fracture cleavages, folds, and joints (modified after Lu et al., 1995).

of the paleostress regimes that have been successively recorded since the late Miocene (Chu, 1990).

The present-day distribution of stress in Taiwan was obtained from the analysis of 1972 to 1986 earthquake focal mechanisms (Fig. 3B) (Yeh et al., 1991). Although a compressional stress regime (with reverse- and strike-slip faulting) dominates in most of Taiwan, results of focal mechanism analyses from northern Taiwan (Fig. 3B) indicate that the present state of stress of this part of the island is compatible with strike-slip and extensional regimes (Yeh et al., 1991).

In summary, all determinations of present-day stress indicated that the regional stress patterns in Taiwan are dominated by (1) northeast-southwest compression in the orogenic belt, due to collision between Eurasia and the Philippine Sea plate, and (2) active north-south and east-west extension in northeasternmost Taiwan and the western tip of the Okinawa Trough (Fig. 3B).

Spatial variation of crustal strain of northern Taiwan

The changes in baseline lengths determined from the repeated GPS surveys in the northern region of Taiwan are used to assess the spatial variation of the horizontal crustal strain over the region. On the basis of a consideration of the geologic structures and the distribution of geodetic stations, northern Taiwan is divided into 17 subnetworks denoted NT1 to NT17 (Fig. 4). Each of these subnetworks includes 4 to 13 GPS stations (Fig. 4). It is assumed that, spatially, the crustal strain accumulates uniformly over each subnetwork (after tensor determination, this assumption is checked by misfit review), and that the rate of strain accumulation is constant over the time period considered (1990–1997). Note that no very large earthquakes—occurred during this period. The maximum magnitude (M_L) was 6.20 so that these data principally reflect the interseismic deformation. Following the procedures of Prescott et al. (1979), the average annual strain rate for each net was calculated for each subnetwork. The strain rate for each baseline, $\dot{e}$, is expressed as $\dot{e} = L^{-1}(dL/dt)$, where L is the baseline length and dL/dt is the average annual strain-rate change. It is related to the surface strain-rate tensor, $\dot{E}ij$, by

$$\dot{e} = \dot{E}_{11}\sin^2\theta + \dot{E}_{12}\sin 2\theta + \dot{E}_{22}\cos^2\theta, \quad (1)$$

where θ is the azimuth (measured clockwise from north) of the baseline and the strain-rate tensor, $\dot{E}ij$, is referred to a geographic coordinate system with axis 1 directed to the east and axis 2 directed to the north. Three components of the average strain-rate tensor, $\dot{E}_{11}$, $\dot{E}_{12}$, and $\dot{E}_{22}$, were thus calculated by using all of the surveys for each of the 17 subnetworks or tectonic blocks (Fig. 4).

The average principal strain rates are computed from three components of the surface strain-rate tensor using the following formula:

$$\dot{\varepsilon}_{1,2} = \tfrac{1}{2}(\dot{E}_{11} + \dot{E}_{22}) \pm [\dot{E}_{12}^{\,2} + \tfrac{1}{4}(E_{11} - \dot{E}_{22})^2]^{1/2}, \quad (2)$$

where ε_1 and ε_2 are the algebraically larger and smaller principal strain rates, respectively. The azimuth of ε_1, φ, is given by

$$\varphi = \tfrac{1}{2}\tan^{-1}[2\dot{E}_{12}/(\dot{E}_{22} - \dot{E}_{11})]. \quad (3)$$

The average principal strain rates for each of the 17 subnetworks are given in Table 1. All uncertainties quoted are ± 1 standard deviation. The strain rates are given in units of microstrain (μstrain) per year (1 μstrain $= 10^{-6}$). Positive values denote extension, whereas negative values represent shortening or contraction.

The most prominent feature of the strain distribution patterns in northern Taiwan certainly corresponds to the Ilan Plain. Significant extension and shortening rates of 0.19 and 0.07/yr in azimuths of 2° and 92°, respectively, are observed in northeastern Taiwan (NT8). The Ilan Plain (NT10) and its eastern offshore area (NT9) show remarkable extension rates of 1.03–1.11 μstrain/yr on an azimuth of 143°–148°. Also in the Ilan Plain (NT10), the largest shortening rate is found (0.77 μstrain/yr with an azimuth of 143°) with a large extension rate in the perpendicular direction (1.13 μstrain/yr with an azimuth of 53°), indicating strike-slip deformation mode. Because this area is considered as a western extension of the Okinawa Trough (Yu and Tsai, 1979; Yeh et al., 1989; Liu, 1995), the extensional deformation is assumed to be related to extension in the Okinawa Trough (Kimura, 1985; Letouzey and Kimura, 1985; Sibuet et al., 1987).

In the northwestern part of Taiwan, insignificant or minor deformations are observed. Overall the shortening rates in this area clearly increase from south to north, which is consistent with the southward propagation of collision and GPS data from the rest of Taiwan (Yu et al., 1997). In the Taipei area, subnetworks NT1–NT4 have small extension rates (0.07–0.15 μstrain/year) and small contraction rates (0.03–0.09 μstrain/year). The extension deformations in these networks mostly trend east-west to east-northeast. Overall, the shortening rates in these areas clearly increase from north to south, which is consistent with the southward propagation of collision and with GPS data of Taiwan (Yu et al., 1997).

FINITE-ELEMENT MODELING

The finite-element technique

The computer code MODULEF was used for the numerical simulation. This finite-element technique was developed by the INRIA (Institut National de Recherche en Informatique et en Automatique) (George et al., 1986). The model used here (Fig. 5) is a two-dimensional model with a plane-stress condition that includes a variety of subdomains with different material properties (Table 2), in order to represent the mechanical behavior

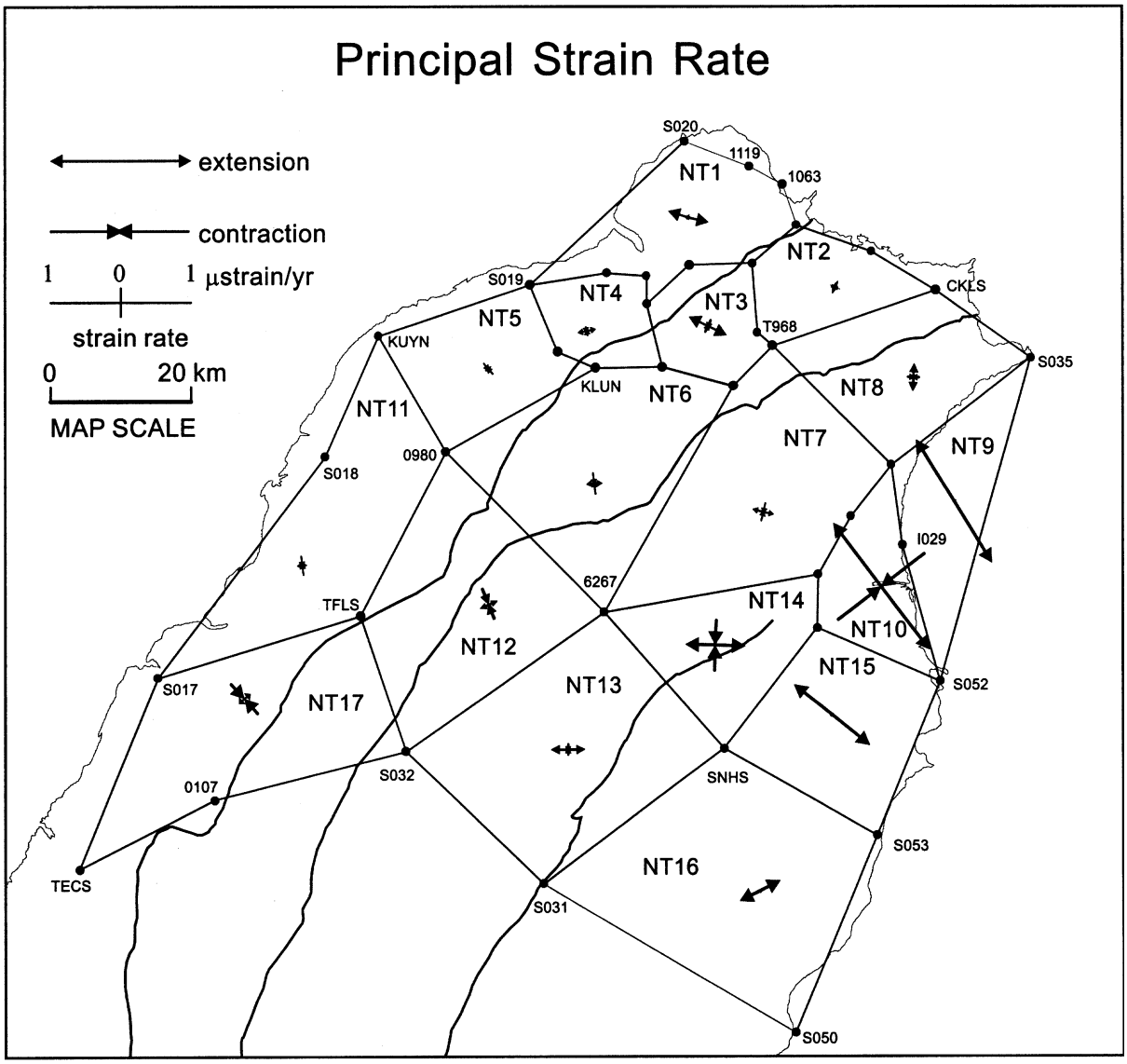

Figure 4. Principal strain rates for 17 subnetworks in northern Taiwan. Thick line denotes contraction, whereas thin line represents extension. Solid circles indicate GPS stations.

of different regions (for details, see Hu et al., 1996). This configuration was chosen according to the regional structural framework of the area under investigation (Fig. 1). As expected for an elastic model that fails to take into account the stress-buffering effects of yielding, purely elastic models produced stresses that were progressively larger and that become unrealistic with increasing amounts of displacements. Owing to the obvious limitations of the elastic model, we adopted an elasto-plastic model with the von Mises criterion, which is more realistic and better accounts for the actual deformation of the mountain belt. With this elasto-plastic model, relatively large deformation can be considered. The elasto-plastic yield limit obviously varies with depth, so that the values adopted represent an average effective yield strength for the model. The depth considered for the brittle deformation is about 20–30 km. Ranalli and Murphy (1987) showed that the depth-dependence of lithospheric rheology varies with tectonic provinces; in many cases the continental lithosphere includes one or two soft ductile layers sandwiched between brittle layers. As a result, brittle behavior may occur either in the upper crust or in the uppermost mantle. In our model, we aim at discussing the brittle deformation in the upper crust through a simplified two-dimensional analysis.

We used plane-stress approximations, which correspond to a two-dimensional model of an "infinitely thin" plate. Under this condition, the vertical component of stress is zero, or is small relative to the horizontal component of stress. The two-dimensional models used may be regarded as the first-order

TABLE 1. GPS-DERIVED PRINCIPAL STRAIN RATES OF 17 SUBNETS IN NORTHERN TAIWAN (1990–1997)

Net	$\dot{E}_1$ (μ strain/yr)	$\dot{E}_2$ (μ strain/yr)	(°)
NT1	0.15 ± 0.02	−0.03 ± 0.02	−74.2 ± 5.5
NT2	0.11 ± 0.04	−0.06 ± 0.04	77.9 ± 9.9
NT3	0.07 ± 0.03	−0.08 ± 0.03	23.0 ± 11
NT4	0.15 ± 0.03	−0.09 ± 0.03	−64.7 ± 5.4
NT5	−0.05 ± 0.03	−0.09 ± 0.03	47.8 ± 33.2
NT6	0.05 ± 0.04	−0.15 ± 0.04	83.7 ± 8.7
NT7	0.09 ± 0.05	−0.12 ± 0.05	−76.9 ± 9.1
NT8	0.19 ± 0.08	−0.07 ± 0.04	1.7 ± 6.5
NT9	1.03 ± 0.06	0.02 ± 0.05	−31.9 ± 3.8
NT10	1.13 ± 0.03	−0.77 ± 0.04	−37.2 ± 0.9
NT11	0.05 ± 0.04	−0.13 ± 0.03	82.2 ± 9.9
NT12	0.09 ± 0.04	−0.21 ± 0.04	67.4 ± 5.8
NT13	0.24 ± 0.06	−0.07 ± 0.06	89.4 ± 5.0
NT14	0.43 ± 0.04	−0.35 ± 0.08	−88.0 ± 3.3
NT15	0.69 ± 0.04	−0.01 ± 0.05	−51.2 ± 3.1
NT16	0.15 ± 0.03	0.01 ± 0.03	64.4 ± 10.7
NT17	0.05 ± 0.02	−0.28 ± 0.04	48.3.7 ± 4.2

TABLE 2. RHEOLOGY AND PARAMETERS USED IN THE FINITE-ELEMENT MODELING

Subdomain	Young's modulus (GPa)	Poisson's ratio	Yield stress (MPa)
S1	60	0.25	300
S2	40	0.25	260
S3	30	0.25	240
S4	10	0.25	240
S5	5	0.25	120
S6	1	0.20	60

Note: Compare with Figure 5.

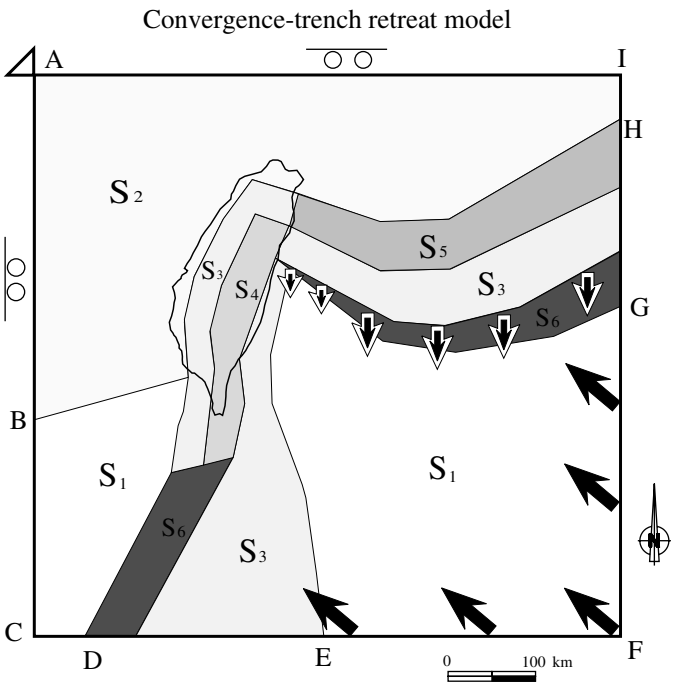

Figure 5. Geometry and boundary conditions of the finite-element model of Taiwan collision. For geographic coordinates, see Figure 1; coast of Taiwan shown as thin dotted line. S_1, S_2, S_3, S_4, S_5, and S_6 are subdomains with different rheologies (Young's modulus, Poisson's ratio, and yield stress listed in Table 2). Uppercase letters A–I indicate segments of frame with different boundary conditions: open triangle—fixed boundary (point A), open circles—roller in one direction (north-south for AB, east-west for AI), no symbol—free segments (BC, CD, DE, IH, and GH). Large black arrows, common direction of displacement based on plate kinematics (EF and FG).

approximation of the problem under consideration; i.e., it does not consider the effects of topography, buoyancy, basal drag, coupling at depth, and thermomechanical deformation within the lithosphere. Another important omission is the possible presence of a mechanically weak layer at mid-crust depth in the continental lithosphere, which could result in mechanical decoupling of the crustal layers. Furthermore, mechanical coupling that may be present in the convergence zone, due to underthrusting oblique to the plate margin, is not considered in our two-dimensional modeling experiments discussed herein.

Geometric configuration of the model and boundary condition

The model covers a rectangular area between latitudes of 19°N and 27°N and between longitudes of 118°E and 127°E (Fig. 5). The 10 subunits of the model represent major structural units according to the regional tectonic setting. Because a rigorous introduction of physically defined parameters for all features is not feasible, the boundaries of the major structural units should be regarded as a first approximation. The model contains 519 triangular linear elements, with three nodes in the summits.

We have used displacement-boundary conditions for the model, because the velocity of plate movement between the Philippine Sea plate and the Eurasian plate is given by the NUVEL-1 global-kinematics results (e.g., Seno et al., 1993) and GPS data (Yu et al., 1997). The northwestern corner of the model is fixed (point A in Fig. 5); displacement is left free along the east-west direction for the northern boundary (AI in Fig. 5) and along the north-south direction for the northwestern boundary (AB in Fig. 5). For the southeastern boundaries of the model (EF and FG in Fig. 5), we imposed an initial horizontal displacement of the plate motion of the Philippine Sea plate relative to Eurasia on the basis of the global plate-kinematic model. The imposed displacement in the models of Figure 5 is 7 cm/yr along the azimuth 310° (Seno et al., 1993). The GPS observed velocity of Lanhsu relative to Paisha is 81.5 ± 1.3 mm/yr, along an azimuth of 306.3° ± 1.2° (Yu et al., 1997), which is slightly larger than the velocity estimated by Seno et al. (1993). We also tried to evaluate the rate of opening of the Okinawa Trough, which influences the deformation field in the northeastern Taiwan area. Letouzey and Kimura (1985) sug-

gested a spreading rate of about 46 mm/yr for the southern Okinawa Trough, based on the study of magnetic anomalies. This rate is consistent with GPS results that reveal a velocity of 56.2 mm/yr along an azimuth of 156° (Fig. 1). It is reasonable to assume that the retreating rate of the Ryukyu Trench is smaller than the opening rate of Okinawa Basin, owing to shortening in the Ryukyu accretionary prism between the Ryukyu arc and the Ryukyu Trench. We consequently adopted a retreating rate of about 15 mm/yr for the model of Figure 6. We set the retreating rate to zero near Taiwan (because the Okinawa Trough extension obviously disappears west of the Ilan Plain), with a linear increase from west to east between 122°E and 123°E (Fig. 5). In order to evaluate the influence of this additional southward displacement of the Ryukyu Trench, we carried out experiments with various velocities. The results obtained with a rate of 15 mm/yr are shown in Figure 6A; the results with a higher rate of 30 mm/yr along the Ryukyu Trench front and 15 km/m.y. near Taiwan are summarized in Figure 6B.

Rheology and material properties

We divided the region studied into 10 subdomains, shown in Figure 5, with six different properties listed in Table 2. The main criteria to define these major rheological properties deal with geologic composition (oceanic crust, continental crust, island-arc crust, foreland belt, metamorphic belt, and accretionary prism), crustal thickness, and thermal state (e.g., the Okinawa Trough area), etc. The materials themselves are considered homogeneous and isotropic. The elastic properties are described by Young's modulus and Poisson's ratio. For the elasto-plastic deformation, a third parameter, the yield stress, is added. The actual values of these parameters are not well determined; as a consequence, we tested models with a variety of values in order to explore the effects of changes in parameters and the sensitivity of our results to various choices. The Young's modulus thus ranges from the highest value in the oceanic lithosphere of the Philippine Sea plate and the South China Sea (S_1 in Fig. 6) to the lowest value in the thinned lithosphere of the Okinawa Trough backarc basin (S_5 in Fig. 5). Intermediate values were assigned to the continental shelf and margin (S_2 in Fig. 5), island arcs (S_3 in Fig. 5), outer and inner mountain belt (S_3 and S_4, respectively, in Fig. 5), and the Okinawa backarc basin (S_5 in Fig. 5). All these values are listed in Table 2. Average Poisson's ratios for the continental and oceanic crusts are taken to be 0.265 and 0.30, respectively (Christensen, 1996), although a Poisson's ratio of 0.25 may be acceptable for common rock types. Abnormally low values of Young's modulus and yield stress were assigned along the subduction zones of the Ryukyu Trench and the Manila Trench (S_6 in Fig. 5). These low values (Table 2) reflect the presence of mechanical decoupling at the trenches. The final values retained in Table 2 may be regarded as somewhat arbitrary. However, numerical experiments revealed that the calculated patterns of stress tra-

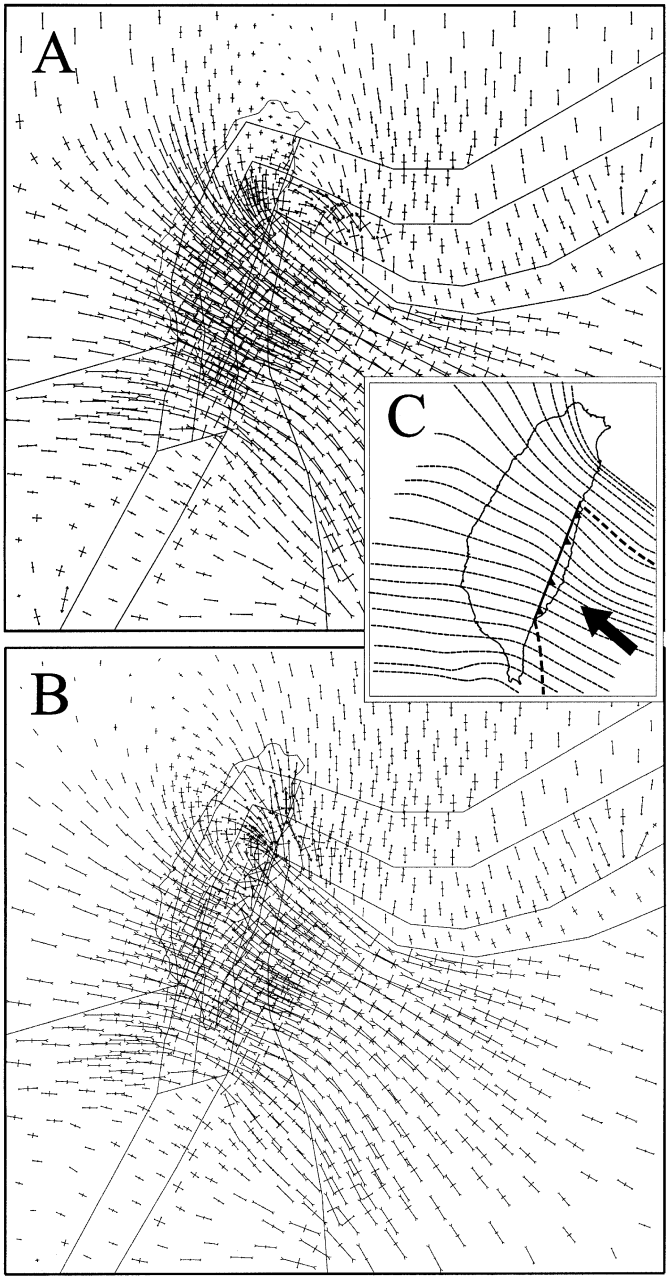

Figure 6. (A) Stress distribution calculated in the convergence and trench-retreat elasto-plastic model. Structure, rheology, and boundary conditions defined in Figure 6. Principal stresses in the horizontal plane shown as small couples of arrows. Pairs of convergent arrows represent maximum compressive stress. Note the stress concentration in the Taiwan collision zone, the fan-shaped distribution throughout the island, and the pronounced stress trajectory deviation near the northwestern corner of the Philippine Sea plate. Pairs of divergent arrows represent minimum extensional stress, especially northeast of Taiwan, in the Okinawa Trough area. (B) Influence of southward trench-retreat velocity. Same explanation as for A except for an increase of southward trench-retreat velocity (see text). Note the westward shift of the transition zone, relative to A. Note also the local occurrence of the east-northeast extensional stress trends in the northeastern Taiwan. (C) Distribution of Quaternary and present-day stresses throughout Taiwan. Main compressional stress field associated with the Quaternary collision from various sources (focal mechanisms, borehole breakouts, and Quaternary fault-slip data). Plate boundary added as thick line with triangles on the hanging wall. Vector of relative plate motion shown by black arrow.

jectories are not sensitive to the values of the assigned elastic constants within a reasonable range of choices.

THE CONVERGENCE AND TRENCH-RETREAT MODEL

The results of the modeling experiments defined in Figure 5 and the previous section are shown in Figures 6 and 7. The fan-shaped distribution of compressional stress trajectories was thoroughly discussed in an earlier paper (Hu et al., 1996). The fan-shaped stress pattern is in agreement with measurements of Quaternary and present-day stresses (Suppe et al., 1985; Barrier and Angelier, 1986; Angelier et al., 1986, 1990; Lee, 1986; Chu, 1990; Yeh et al., 1991), as summarized in Figure 6C. Figures 6 and 7 also show the importance of north-south extensional stress in the Okinawa Trough–Ryukyu arc region, which is consistent with the seismotectonic data available in the western Ryukyu arc and the Ilan Plain (Yeh et al., 1991; Kao et al., 1998). Our model predicts that a transitional regime in northeastern Taiwan exists between the pure compressional tectonic regime in the collision zone of Taiwan and the extensional tectonic regime in the northeastern part of the Taiwan. Furthermore, the transition in the stress field, where significant strike-slip deformation can be expected, is characterized by two intermediate subregimes: one is mostly compressional, the other one is mostly extensional, as indicated by patterns of crosses and triangles, respectively, in Figure 7. From west to east across the transition zone, the relative magnitudes of stress vary from compression to extension (Fig. 7).

An interesting conclusion of the experiments lies in the significant migration of the transition zone as boundary conditions vary. A simple increase in the velocity of the southward retreat of the subduction zone (30 mm/yr in Fig. 7B in stead of 15 mm/yr in Fig. 7A) results in a southwestward shift of more than 50 km of the transition zone (compare Fig. 7, A and B). Thus the transition between regional compression (Taiwan collision belt) and extension (Okinawa-Ryukyu system) is extremely sensitive to variations in boundary conditions. The general influence of these changes is shown in Figure 6, A and B, with same boundary conditions as for Figure 7, A and B, respectively, showing that the pattern of compressional stress in the collision belt of central and southern Taiwan undergoes little perturbation. In other words, the high sensitivity of the stress regimes to the variations in trench retreat is restricted to northern Taiwan. To the south, these effects sharply diminish and practically vanish in the southern half of Taiwan (Fig. 6). We conclude that the effects of the suction force related to the Ryukyu subduction zone play a very important role in northern Taiwan, but have very little influence farther south, in most of the collision zone.

DISCUSSION

The finite-element models presented herein are significantly simplified with respect to the actual structure and tec-

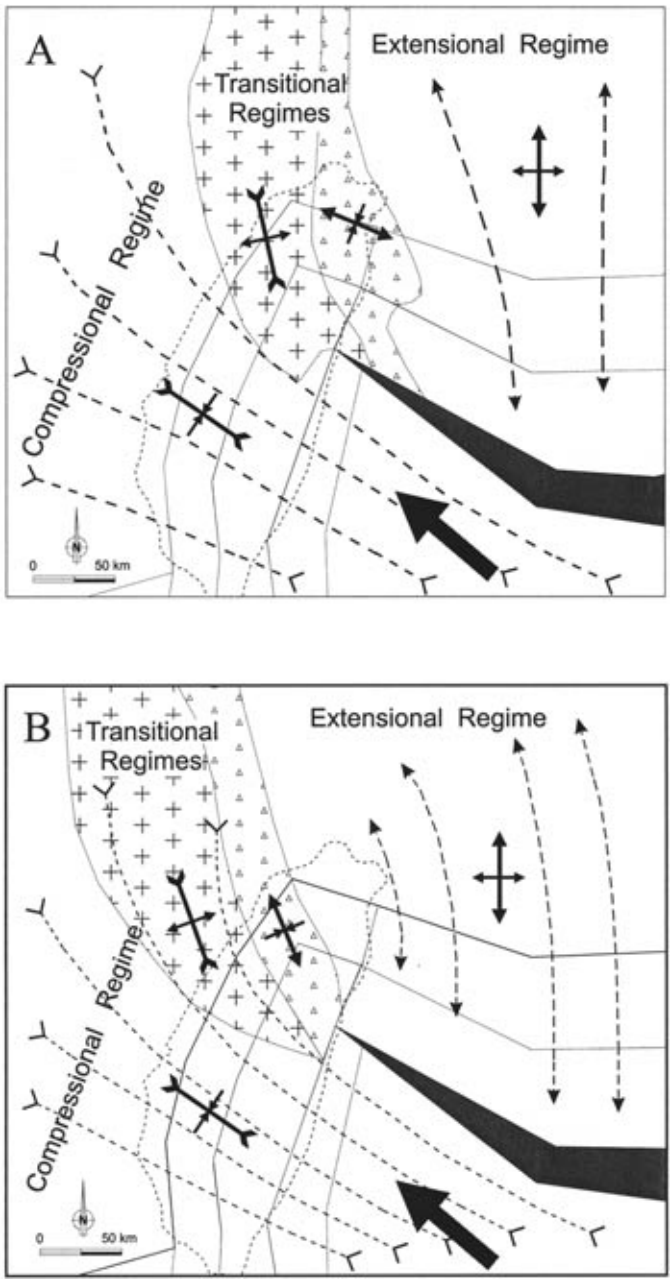

Figure 7. (A) Resulting tectonic regimes and the trajectories of σ_1, based on model shown in Figure 6A (see Table 2). Dashed lines with convergent arrowheads indicate compressional trajectories in the area of pure compression. Dashed lines with divergent arrowheads indicate extensional trajectories in the area of pure extension. Pairs of convergent arrows represent maximum compressive stress. Pairs of divergent arrows represent minimum extensional stress. Open triangles—regions of transtension. Crosses—regions of transpression. Zone of decoupling in dark gray. Vector of relative plate motion as black arrow. (B) Schematic stress patterns, σ_1 trajectories, and σ_3 trajectories correspond to the model shown in Figure 6B. Note that the main difference, relative to Figure 6A, is a westward shift of the transition from compression (Taiwan) to extension (Ryukyu).

tonism in and around Taiwan. However, they provide a mechanically consistent framework (Fig. 5) for interpreting the observed stress and strain patterns (Figs. 3 and 4), in relation to the major features and kinematics of this collision-subduction area. The interaction between opening of the Okinawa Trough and the collision of eastern Taiwan plays a crucial role in determining the regional stress patterns (e.g., Hu et al., 1996; Teng and Lee, 1996). Teng (1996) suggested that the orogenic collapse of northern Taiwan is mainly triggered by the change in the boundary forces induced by the change in vergence of subduction. According to this interpretation, the continental margin of southern Ryukyu and northern Taiwan first underwent a lithospheric thickening, as induced by collision, which was followed by lithospheric stretching, as induced by trench suction. This general idea was proposed by Viallon et al. (1986) based on numerical modeling and by Teng (1996) based on qualitative approach.

Our numerical simulation indicates that the crustal deformation in the Ryukyu-Taiwan area may be strongly affected by the interaction between the indentation of the Philippine Sea plate and the suction at the Ryukyu Trench (Fig. 5). This interaction results in a varying stress-strain field. Three subregimes may be distinguished: a compressional regime in south-central Taiwan, an extensional regime in northeast Taiwan and south Ryukyu, and, between these domains, a transition zone with transtension and transpression subdomains. The transition zone migrates significantly as a function of the variable ratios between velocities of northwest-southeast convergence and north-south trench retreat.

Our numerical models also predict that the maximum tension in the Okinawa Trough area rotates counterclockwise from north-south to northwest-southeast, with magnitudes that decrease as one approaches northeast Taiwan (Figs. 6 and 7). Similarly, the trends of the maximum compression in central Taiwan gradually turn clockwise from northwest-southeast to north-south and even to northeast-southwest as one approaches northeast Taiwan, while the magnitudes decrease rapidly.

The transition zone between these different tectonic regimes coincides with the area where the Okinawa seismic zone, the interface seismic zone, the collision seismic zone, and the lateral-compression seismic zone merge (Kao et al., 1998). The observation of sharp changes in the trends of minimum stress, from approximately north-south in the Ilan Plain and Okinawa Trough to approximately east-west in northernmost Taiwan supports our numerical simulation. The model is also supported by the distribution of earthquake focal mechanisms in this area (Kao et al., 1998). The S waveform's splitting observed in northern Taiwan, interpreted to be caused by stress-aligned cracks in the upper crust (Kuo et al., 1994), is consistent with the present conclusion that northeastern Taiwan is currently under the combined actions of extension due to the Okinawa Trough opening and compression due to the collision between the Philippine Sea plate and Eurasia.

Lu and Malavieille (1994) used three-dimensional sand-box-modeling experiments to illustrate the kinematic processes of the Taiwan thrust wedge. The results showed a major consequence of oblique collision with an asymmetric indenter in the development of an asymmetric thrust wedge with a characteristic distribution of tectonic domains. The deformation within the belt is a combination of shortening, rotations, and stretching, which locally results in a partitioning among thrusting, strike-slip faulting, and normal faulting. On the basis of these results, Lu et al. (1995) suggested that the northeastern segment of the Taiwan belt (Fig. 8) first underwent contractional deformation (such as shortening and oblique thrust-sheet stacking), followed by right-lateral transcurrent faulting and normal faulting. Lu et al. (1995) pointed out that the indentation results not only in contractional tectonics across the belt (Fig. 8A), but also in divergent strike-slip components and block rotation as well as local occurrence of extension roughly parallel to the trends of the major units of the belt (Fig. 8A). These authors concluded that extensional structures such as the Taipei Basin developed in response to increasing belt curvature and related block rotations (Fig. 3A), and, due to the asymmetry of the collision (Fig. 8B), the amounts of right-lateral strike slip and clockwise rotation east of the Tanshui River axis (Fig. 8A) are larger than those of the left-lateral strike slip and counterclockwise rotation west of it (Fig. 8B). These interpretations were supported not only by tectonic analyses but also by paleomagnetic reconstruction of rotation in northern Taiwan (Lee et al., 1991; Lue et al., 1991). The presence of nearly east-west extension in northeasternmost Taiwan (Fig. 3) is also in good agreement with the reconstruction in Figure 8.

The complex deformation of northern Taiwan, however, cannot be accounted for solely by the effects of wedge convergence. Northeast off Taiwan, the Okinawa Trough area is dominated by extensional tectonics (Kimura, 1985; Letouzey and Kimura, 1985, 1986; Sibuet et al., 1987) as a result of the suction force related to the Ryukyu Trench retreat. Part of the extensional regime present in northeastern Taiwan, especially for the north-south extension near the Ilan Plain (Tsai, 1986; Yeh et al., 1989, 1991), is the westernmost expression of the slab-related backarc extension. Hu et al. (1996) confirmed that the extension in the Ryukyu arc and the western Okinawa Trough cannot be explained solely by lateral extrusion, as a simple consequence of the Taiwan collision. Here we point out that the suction force related to the southward retreat of the Ryukyu subduction zone may play a major role.

CONCLUSION

The study of two-dimensional elasto-plastic finite-element modeling of the subduction-collision in and around Taiwan allows us to estimate the influences of different parameters in producing the stress and strain patterns. The main constraints for testing the model experiments are derived from both the tectonic and seismic studies and the GPS analyses of Taiwan deformation. Additional constraints are provided by consider-

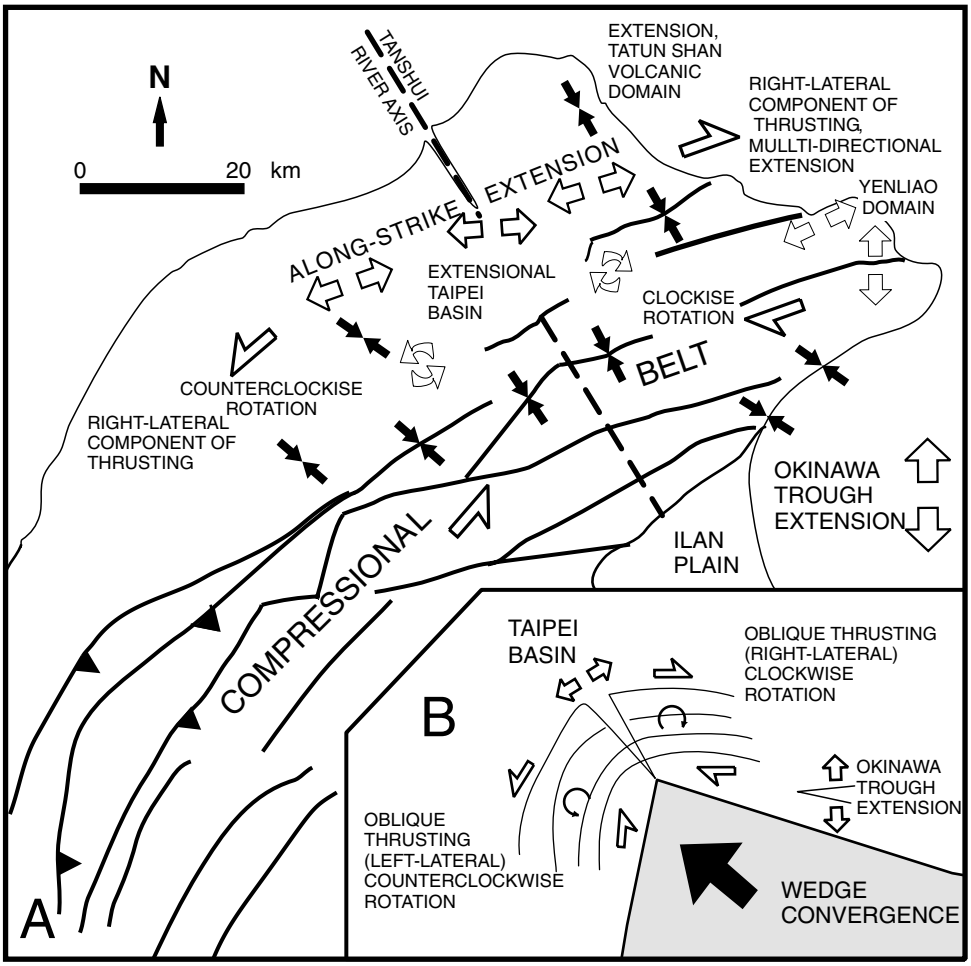

Figure 8. (A) Interpretative map and (B) explanatory sketch. Model of Pliocene–Quaternary tectonic deformation in the foreland thrust belt of northern Taiwan (modified after Lu et al., 1995). Note the existence of three major domains: (1) the eastern domain with right-lateral oblique-slip thrusting, right-lateral strike-slip, and clockwise rotations; (2) the central domain characterized by indentation in the inner belt and extensional deformation in the outer belt; and (3) the western domain with left-lateral oblique thrusting, right-lateral strike-slip, and counterclockwise rotations. Explanation of symbols in A.

ation of structural geology and paleomagnetic results. According to our two-dimensional numerical simulations, the crustal deformation in the Ryukyu-Taiwan area is controlled by two major factors: the indentation of the Philippine Sea plate into Eurasia and the trench retreat due to suction at the Ryukyu Trench (Fig. 6). The interaction of these two forces results in a complex stress-strain field that includes a compressional regime in south-central Taiwan, an extensional regime in northeast Taiwan and south Ryukyu, and a narrow transitional regime in between. The interaction between the opening of the Okinawa Trough and the collision along eastern Taiwan may play a crucial role in determining the regional stress and strain patterns, and its variations resulted in significant migration of the transition zone (Fig. 7).

The westward migration of the Okinawa Trough seems to be the reason for increasing intensity of extension with time in northern Taiwan. According to recent studies (Chung et al., 1995; Chen et al., 1995), the eruption of Quaternary andesitic volcanic rocks in this area is probably a result of the change in stress field from pure compression to extension. The interaction already discussed can explain the spatial clockwise rotation of stress axes from northwest-southeast to nearly north-south compression, then progressively to east-west extension and finally to north-south extension. The migration of the Okinawa Trough system and the variations in time of the two sources can explain the local successions of stress regimes, although the ages of the tectonic events are poorly determined (Figs. 6 and 7). Our numerical models predicted that the maximum tension in the Okinawa Trough rotates significantly from north-south to northwest-southeast, and magnitudes decrease rapidly toward northeast Taiwan (Fig. 6). The trajectory of the maximum compression follows the relative convergence direction along the Longitudinal Valley, but gradually turns to northeast-southwest with decreased magnitude in northeast Taiwan. The transition zone between these two stress regimes coincides with the place where the major seismogenic structures merge.

ACKNOWLEDGMENTS

We are grateful to L. Royden, C. Wang, and T. Byrne for constructive and helpful reviews of the manuscript. This research was financially supported by Academia Sinica and the National Science Council of the Republic of China under grant NSC 86-2116-M-001-025. Thanks are due to our colleagues C.-H. Yen

and H.-H. Su for their assistance in preparing this manuscript and the illustrations. This work is also part of the Taiwan-France cooperation framework supported by the NSC and the French Institute in Taipei. Some figures are generated by the GMT software written by Paul Wessel and Walter H.F. Smith.

REFERENCES CITED

Angelier, J., 1990, Foreword, Geodynamics of the eastern Eurasian Margin: Tectonophysics, Special Issue, v. 183, p. vii-x.

Angelier, J., Barrier, E. and Chu, H.-T., 1986, Plate collision and paleostress trajectories in a fold-and thrust belt: The Foothills of Taiwan: Tectonophysics, v. 125, p. 161–178.

Angelier, J., Bergerat, F., Chu, H.-T. and Lee, T.-Q., 1990, Tectonic analysis and the evolution of a curved collision belt: The Hsüehshan Range, northern Taiwan: Tectonophysics, v. 183, p. 77–96.

Barrier, E., 1985, Tectonique d'une chaîne de collision active: Taiwan: Paris, Université de Pierre et Marie Curie, Mém. Sci. Terre, no. 85–29, 492 p.

Barrier, E., 1986, The double collision of Taiwan: An active orogen: Tectonophysics, v. 125, p. 39–72.

Barrier, E. and Angelier, J., 1986, Active collision in eastern Taiwan: The Coastal Range: Tectonophysics, v. 125, p. 39–72.

Biq, C., 1989, The Yushan-Hsüehshan megashear zone in Taiwan: Proceedings of the Geological Society China, v. 32, p. 7–20.

Chen, C.-H., Lee T., Shieh Y.-N., Chen, C.-H., and Hsu, W.-Y., 1995, Magmatism at the onset of back-arc basin spreading in the Okinawa Trough: Journal of Volcanology and Geothermal Research, v. 69, p. 313–322.

Christensen, N.I., 1996, Poisson's ratio and crustal seismology: Journal of Geophysical Research, v. 101, p. 3139–3156.

Chu, H.-T., 1990, Néotectonique cassante et collision plio-quaternaire à Taiwan: Paris, Université Pierre et Marie Curie, Mém. Sci. Terre, no. 90–28, 292 p.

Chung, S.-L., Yang, T.F., Lee, C., and Chen, C.-H., 1995, The igneous provinciality in Taiwan: Consequence of continental rifting superimposed by Luzon and Ryukyu subduction systems: Journal of Southeast Asian Earth Sciences, v. 11, p. 73–80.

Clark, M.B., Fisher, D.M., Lu, C.-Y., and Chen, C.-H., 1993, Kinematic analysis of the Hsüehshan Range, Taiwan: A large-scale pop-up structure: Tectonics, v. 1, 1153–1172.

Dixon, T.H., 1991, An introduction to the Global Positioning System and some geological applications: Review of Geophysics, v. 29, p. 249–276.

George, P.L., Laug, P., Muller, B., and Vidrascu, M., 1986, Guide d'utilisation et normes de programmation: Le Chesnay, France, Institute de National Recherche Informatique Automatique, 113 p.

Ho, C.-S., 1986, A synthesis of the geologic evolution of Taiwan: Tectonophysics, v. 125, p. 1–16.

Hu, J.-C., Angelier, J., Lee, J.-C., Chu, H.-T., and Byrne, D., 1996, Kinematics of convergence, deformation and stress distribution in the Taiwan collision area: 2-D finite-element numerical modeling: Tectonophysics, v. 255, p. 243–268.

Hu, J.-C., Angelier J., and Yu, S.-B., 1997, An interpretation of the active deformation of southern Taiwan based on numerical simulation and GPS studies: Tectonophysics, v. 274, p. 145–170.

Huchon, P., Barrier, E., De Bremaecker, J.C., and Angelier, J., 1986, Collision and stress trajectories in Taiwan: A finite element model: Tectonophysics, v. 125, p. 179–191.

Kao, H., and Chen, W.-P., 1991, Earthquakes along the Ryukyu-Kyushu arc: Strain segmentation, lateral compression, and the thermomechanical state of the plate interface: Journal of Geophysical Research, v. 96, p. 21443–21485.

Kao, H., Shen, S.-J., and Ma, K.-F., 1998, Transition from oblique subduction to collision: Earthquakes in the southernmost Ryukyu arc-Taiwan Region: Journal of Geophysical Research, v. 94, p. 17561–17579.

Kimura, M., 1985, Back-arc rifting in the Okinawa Trough: Marine Petroleum Geology, v. 2, p. 222–240.

Kuo, B.-Y., Chen, C.-C., and Shin, T.-C., 1994, Split S waveforms observed in northern Taiwan: Implication for crustal anisotropy: Geophysical Research Letters, v. 21, p. 1491–1494.

Lacombe, O., Angelier, J., Chen H.-W., Deffontaines, B., Chu, H.-T., and Rocher, M., 1997, Syndepositional tectonics and extension-compression relationships at the front of the Taiwan collision belt: A case study in the Pleistocene reefal limestones near Kaohsiung, SW Taiwan: Tectonophysics, v. 274, p. 109–120.

Lee, C.-T., 1986, Methods of stress analysis and paleostress changes in northern Taiwan due to arc-continent collision [Ph.D. thesis]: Taipei, National Taiwan University, 370 p.

Lee C.-T., and Wang Y., 1988, Quaternary stress changes in northern Taiwan and their tectonic significance: Proceedings of the Geological Society of China, no. 31, p.154–168.

Lee, T.-Q., Angelier, J., Chu, H.-T., and Bergerat, F., 1991, Rotations in the northern eastern collision belt of Taiwan: Preliminary results from paleomagnetism: Tectonophysics, v. 199, p. 109–120.

Letouzey, J., and Kimura, M., 1985, The Okinawa Trough genesis, structure and evolution of a back-arc basin developed in a continent: Marine Petroleum Geology, v. 2, p. 111–130.

Letouzey, J., and Kimura, M., 1986, The Okinawa Trough: Genesis of a back-arc basin developing along a continental margin: Tectonophysics, v. 125, p. 209–230.

Liew, P.-M., Hsieh, M.-L., and Lai, C.-K, 1990, Tectonic significance of Holocene marine terraces in the Coastal Range, eastern Taiwan: Tectonophysics, v. 183, p. 121–127.

Liu C.-C., and Yu, S.-B., 1990, Vertical crustal movements in eastern Taiwan and their tectonic implications: Tectonophysics, v. 183, p. 111–119.

Liu, C.-C., 1995, The Ilan Plain and the southwestward extending Okinawa Trough: Journal of Geological Society of China, v. 38, p. 229–242.

Liu, C.-S., Lundberg, N., Huang, I.L., and Teng, L.S., 1997, Structure features off southwestern Taiwan: Marine Geology, v. 137, p. 305–319.

Lu, C.-Y., and Malavieille, J., 1994, Oblique convergence indentation and rotation tectonics in the Taiwan Mountain Belt: Insights from experimental modeling: Earth and Planetary Science Letters, v. 121, p. 474–494.

Lu, C.-Y., Angelier, J., Chu, H.-T., and Lee, J.-C., 1995, Contractional, transcurrent, rotational and extensional tectonics: Examples from Northern Taiwan: Tectonophysics, v. 125, p. 129–146.

Lue, Y.-T., Lee, T.-Q., Horng, C.-S., and Wang, Y., 1991, Magnetic fabric in the non-metamorphosed terrain of the northwestern Foothills-Hsüehshan belts of Taiwan: Proceedings of the Geological Society of China, no. 34, p. 131–146.

Mars Inc., 1981, Radar mosaic image of northern Taiwan (sheet 1, south looking direction): Taipei, Taiwan, MRSO, Industrial Technology Research Institute, Mars Contract, 78086.

Pezzopane, S.K., and Wesnousky, S.G., 1989, Large earthquakes and crustal deformation near Taiwan: Journal of Geophysical Research, v. 94, p. 7250–7264.

Pirazzoli, P.A., Arnold, M., Giresse, P., Hsieh, M.-L., and Liew, P.-M., 1993, Marine deposits of late glacial times exposed by tectonic uplift on the east coast of Taiwan: Marine Geology, v. 110, p. 1–6.

Prescott, W.H., Savage, J.C., and Kinoshita, W.T., 1979, Strain accumulation rates in the western United States between 1970 and 1978: Journal of Geophysical Research, v. 86, p. 6067–6072.

Ranalli, G., and Murphy, D., 1987, Rheological stratification of the lithosphere: Tectonophysics, v. 132, p. 281–295.

Rocher, M., Lacombe, O., Angelier, J., and Chen, H.-W., 1996, Mechanical twin sets in calcite as markers of recent collisional events in a fold-and-thrust belt: Evidence from the reefal limestones of southwestern Taiwan: Tectonics, v. 15, p. 984–996.

Sato, T., Koresawa, S., Shiozu, Y., Kusano, F., Uechi, S., Nagaoka, O., and Kasahara, J., 1994, Microseismicity of back-arc rifting in the middle Okinawa Trough: Geophysical Research Letters, v. 21, p. 13–16.

Seno, T., Stein, S., and Gripp, A.E., 1993, A model for the motion of the Philippine Sea plate consistent with NUVEL-1 and geological data: Journal of Geophysical Research, v. 98, p. 17941–17948.

Sibuet, J.-C., Letouzey, J., Barbier, F., Charvet, J., Foucher, J.P., Hilde, T.W.C., Thomas, W.C., Kimura, M., Chiao, L.-Y., Marsset, B., Muller, C., and Stephan, J.F., 1987, Back arc extension in the Okinawa trough: Journal of Geophysical Research, v. 92, p. 14041–14063.

Sibuet, J.-C., Deffontaines B., Hsu, S.-K., Thareau, N., Formal, J.-P., Liu, C.-S., and ACT party, 1998, Okinawa trough backarc basin: Early tectonic and magmatic evolution: Journal of Geophysical Research, v. 103, p. 30245–30267.

Suppe, J., 1984, Kinematics of arc-continent collision, flipping of subduction and back-arc spreading near Taiwan: Memoir of the Geological Society of China, v. 6, p. 21–33.

Suppe, J., Hu, C.-T., and Chen, Y.-J., 1985, Present-day stress direction in western Taiwan inferred from borehole elongation: Petroleum Geology of Taiwan, n. 21, p. 1–12.

Teng, L.S., 1990, Geotectonic evolution of late Cenozoic arc-continent collision in Taiwan: Tectonophysics, v. 183, p. 57–76.

Teng, L.S., Chen, C.-H., Wang, W.-S., Liu, T.-K., Jung, W.-S., and Chen, J.-C., 1992, Plate kinematic model for Late Cenozoic arc magmatism in northern Taiwan: Journal of Geological Society of China, v. 35, p. 1–18.

Teng, L.S., 1996, Extensional collapse of the northern Taiwan mountain belt: Geology, v. 24, p. 949–952.

Teng, L.S., and Lee, C.-T., 1996, Geomechanical appraisal of seismogenic faults in northeast Taiwan: Extensional collapse of the northern Taiwan mountain belt: Journal of the Geological Society of China, v. 39, p. 125–142.

Tsai, Y.-B., Teng, T.L., Chiu, J.-M., and Liu, H.-L., 1977, Tectonic implications of the seismicity in the Taiwan region: Memoir of the Geological Society of China, v. 2, p. 13–41.

Tsai, Y.-B., 1986, Seismotectonics of Taiwan: Tectonophysics, v. 125, p. 17–37.

Viallon, C., Huchon, P., and Barrier, E., 1986, Opening of the Okinawa basin and collision in Taiwan: A retreating trench model with lateral anchoring: Earth and Planetary Science Letters, v. 80, p. 145–155.

Wang, C.-H., and Burnett, W.C., 1990, Holocene mean uplift rates across an active plate collision boundary in Taiwan: Science, v. 248, p. 204–206.

Wu, F.T., 1978, Recent tectonics in Taiwan: Journal of Physical Earth, v. 26, p. s265–s299.

Yeh, Y.-H., Lin, C.-H., and Roecker, S.W., 1989, A study of upper crustal structures beneath northeastern Taiwan: Possible evidence of the western extension of Okinawa Trough: Proceedings of the Geological Society of China, no. 32, p. 139–156.

Yeh, Y.-H., Barrier, E., Lin, C.-H., and Angelier, J., 1991, Stress tensor analysis in the Taiwan area from focal mechanisms of earthquakes: Tectonophysics, v. 200, p. 276–280.

Yu, S.-B., and Tsai, Y.-B., 1979, Geomagnetic anomalies of the Ilan Plain, Taiwan: Petroleum Geology of Taiwan, no. 16, p. 19–27.

Yu, S.-B., and Chen, H.-Y., 1994, Global positioning system measurement of crustal deformation in the Taiwan arc-continent collision zone: TAO, Terrestrial, Atmospheric and Oceanic Sciences, v. 5, p. 477–498.

Yu, S.-B., Chen, H.-Y., and Kuo, L.-C., 1997, Velocity field of GPS Stations in the Taiwan area: Tectonophysics, v. 274, p. 41–59.

Manuscript Accepted by the Society

Printed in the U.S.A.